Quantitative determination of species production from phenol-formaldehyde resin pyrolysis

Hsi-Wu Wong*

Department of Chemical Engineering
University of Massachusetts Lowell, Lowell, MA 01854

Jay Peck, Robin E. Bonomi, James Assif

Center for Aero-Thermodynamics
Aerodyne Research, Inc., Billerica, MA 01821

Francesco Panerai

Department of Mechanical Engineering
University of Kentucky, Lexington, KY 40506

Guillaume Reinisch

Center for Predictive Engineering and Computational Sciences
University of Texas at Austin, Austin, TX 78712

Jean Lachaud

University Affiliated Research Center
University of California at Santa Cruz, Moffett Field, CA 94035

Nagi N. Mansour

NASA Ames Research Center, Moffett Field, CA 94035

Abstract

Batch pyrolysis of a commercial resole type phenol-formaldehyde resin was performed using a step-wise heating procedure in a temperature increment of 50 K from 320 to 1290 K. A resin sample of 50 mg was loaded in a

---

*Corresponding author
  Email address: HsiWu_Wong@uml.edu (Hsi-Wu Wong)

reactor assembly specifically designed and built for this study. Mass loss was measured after each 50 K step and the production of pyrolysis products was quantified using gas chromatography techniques. The overall mass loss from the samples reached 39.2% after the entire procedure. Three major product families were identified: 1) water is the most dominant product at a pyrolysis temperature below 800 K; 2) phenol derivatives (aromatic alcohols) have significant yields at a pyrolysis temperature between 500 and 850 K; 3) permanent gases such as hydrogen, methane, carbon monoxide, and carbon dioxide have the highest yields at a temperature above 800 K. Minor products observed include aromatics, which are formed between 700 and 850 K, and C_2 to C_4 light hydrocarbons, which are only formed above 800 K and peak at 1000 K.

1. Introduction

Pyrolysis of phenol-formaldehyde resins is one of the most common processes to produce amorphous carbon or carbon/carbon composites [1–4]. During pyrolysis, resin matrix converts into carbon, releasing gaseous products. The internal pressure generated from these pyrolysis products, however, poses a potential threat to the structure of carbon/carbon composites [2–4]. For this reason, one needs to obtain a detailed undestanding of the decomposition kinetics of phenol-formaldedyde resins to harness the process. Similarly, when designing ablative and friction materials using phenol formaldehyde resins for aerospace applications, in-depth knowledge of the

11　pyrolysis kinetics is also essential for obtaining optimal performance and ac-
12　curate materials response predictions [5–9] .

13　　Many experimental studies have been performed to understand the py-
14　rolysis kinetics of phenol-formaldehyde resins. Three families of techniques
15　have been used. Thermal analytical techniques, including thermogravimet-
16　ric analysis (TGA), differential scanning calorimetry (DSC), or differential
17　thermogravimetry (DTG), provide sample weight loss and heat flow infor-
18　mation as a function of temperature [2, 3, 10–15]. These methods, although
19　valuable in determining the enthalpies of the pyrolysis reactions and the over-
20　all mass loss, do not give detailed speciation information, necessary for the
21　construction of detailed pyrolysis reaction mechanisms. Infrared (IR) spec-
22　troscopy techniques, such as Fourier transform infrared spectroscopy (FTIR),
23　are used to analyze structural changes of the phenolic resin during pyrolysis
24　[1, 4, 12, 15–20]. Qualitative or semi-quantitative speciation information can
25　be derived, especially coupled with thermal analytical methods, but it is dif-
26　ficult to obtain quantitative product yields over a wide temperature range.
27　Gas chromatography (GC) techniques, such as pyrolysis gas chromatography
28　mass spectrometry (Py-GC-MS) [4, 13, 19, 21–26], provide detailed specia-
29　tion information. However, introduction of the pyrolysis products into the
30　GC systems without loss is challenging, especially for high temperature reac-
31　tions where condensation of the volatile products is suspected to take place
32　in the transfer lines.

33　　Although experimental limitations exist, it is generally accepted that py-
34　rolysis of phenol-formaldehyde resins can be divided into three major stages,
35　as proposed by Trick et al. [1, 2]. The first stage involves crosslink formation

3

36 as a result of condensation reactions to produce water and heavier aromatic

37 species, which takes place in a temperature range between 550 and 800 K.

38 The second stage involves crosslink breaking, forming light gases, such as

39 methane, carbon monoxide and carbon dioxide, in a temperature range be-

40 tween 700 and 1100 K. The last stage involves the charring of the remaining

41 resin through the formation of hydrogen gas at a temperature above 850 K.

42 While these stages generally explain available experimental findings in the

43 literature, a detailed chemical kinetic mechanism that can quantitatively ex-

44 press the temperature-dependent species production of phenol-formaldehyde

45 resin pyrolysis is still lacking. One of the key challenges is limited available

46 data on the detailed and quantitative species production under a wide range

47 of conditions, such as reaction temperature.

48 Only few experimental studies attempted to quantitatively determine

49 yields of detailed pyrolysis products over a wide range of temperature. The

50 experiment performed by Sykes [21] more than 40 years ago remains to be the

51 one with the most comprehensive data. In Syke's study, phenol-formaldehyde

52 resin samples were heated in a pyrolyzer attached to the entrance port of a

53 gas chromatograph. Approximately 7 mg of material was heated for 10 sec-

54 onds before the sample was immediately quenched. The starting temperature

55 was 298 K, and it was increased by 50 K every time when the process was re-

56 peated. Mole fractions of the gaseous products were determined as a function

57 of temperature, as reproduced in Figure 1.

58 In this work, we provide a comprehensive, quantitative speciation data set

59 for phenol-formaldehyde resin pyrolysis over a wide range of reaction temper-

60 ature (320–1290K). We employed gas chromatography methods because they
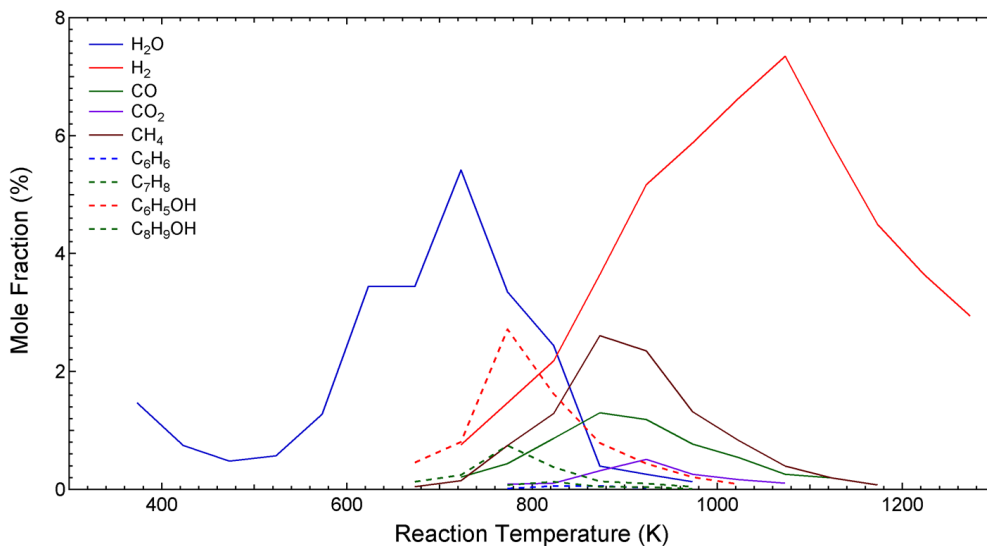
4

Figure 1: Product distribution from the decomposition of a phenolic formaldehyde resin at a heating rate of 10 K/min, reported by Sykes [21].

61 are the most promising for species identification and quantification according
62 to previous literature studies. Thermogravimetric analysis results were also
63 used for comparison. To overcome known limitations of the GC techniques,
64 we designed and constructed a batch reactor system. The uniqueness of our
65 reactor system is that everything produced in the reactor was collected with-
66 out loss and was quantitatively analyzed, thus avoiding the issue of sample
67 loss in typical GC techniques. Our work provides critical information to
68 advance the understanding of reaction kinetics of phenol-formaldehyde resin
69 pyrolysis. The design of this original reactor system and the results of the py-
70 rolysis experiments performed using this set-up are presented in the following
71 sections.

2. Experimental techniques

2.1. Reactor Design

A batch reactor system was designed and built to carry out the pyrolysis experiments. The design of the reactor assembly is shown in Figure 2. The reactor section was made of quartz, taking advantage of its high temperature capability and good thermal shock resistance. The rest of the reactor system was made of stainless steel. Two thermocouples were used to monitor and record temperatures; one inside the sample and the other at the reactor top near the interface between the quartz reactor and the stainless steel fitting. During the experiments, the quartz reactor was inserted into a heating furnace, custom-made from high-temperature heating wires and castable ceramics, as shown in Figure 3. The furnace temperature was controlled with a PID controller. The condenser was positioned in a liquid nitrogen bath, allowing the pyrolysis products to move toward the condenser section by thermal diffusion, where most volatile species condense. The reactor system was designed to cool down as quickly as possible outside the reaction zone. Lower temperature outside the reaction zone also reduces system pressure and allows larger species with low volatility to condense, both of which lower the effect of homogeneous gas phase chemistry.

2.2. Experimental procedure

The experimental protocol employed in this study partially replicated the protocol used by Sykes [21]. The main goal is to store and analyze pyrolysis products within 50 K temperature increments (that is, between 320 and 370 K, 370 and 420K, etc.) rather than attempting on-the-fly measurements,
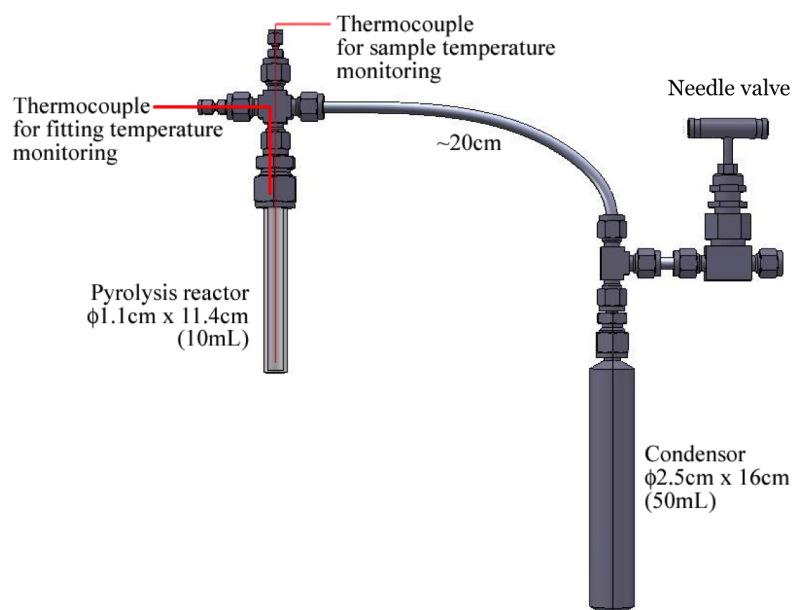
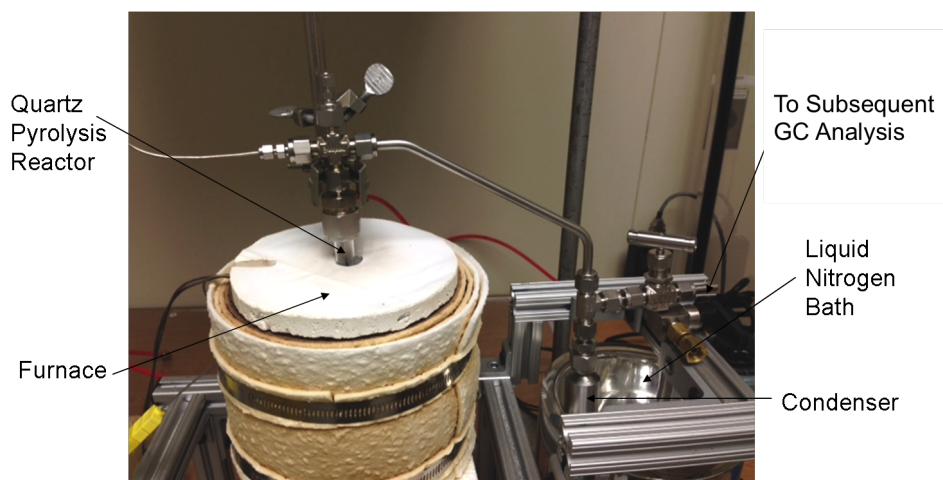Figure 2: 3D model of the batch reactor with key dimensions.

Figure 3: The batch reactor system for the phenolic pyrolysis experiments.

which are susceptible to sample loss due to condensation of pyrolysis products in the reactor and transfer lines. There are two advantages to our approach: (1) the sample's mass can be measured at each step, avoiding the need of using a thermogravimetric analyzer where volatile vapors may condense in the system, and (2) the volatile pyrolysis products that condense on the wall of the reactor assembly can be easily collected by liquid extraction and analyzed.

Resole type phenol-formaldehyde resin samples acquired from Durez Corporation were firstly cured at 450 K for 30 minutes (as instructed by the sample supplier). 50 mg of cured samples were loaded in the quartz reactor. The reactor was then vacuumed to below 13 pascals (0.1 torr) to minimize any potential gas-phase chemistry. The needle valve of the reactor was then closed, and the reactor assembly was inserted into the furnace pre-set at a desired reaction temperature. The sample typically reached the furnace temperature within 2 to 10 minutes following insertion. The reactor was kept at the target temperature for one hour to ensure that pyrolysis reactions at this temperature were near completion. The reactor was then quenched in a cold water bath back to room temperature, typically within two minutes. Examples of measured sample temperature as a function of time during our experiments can be seen in Figure 4.

The internal pressure in the reactor after the reaction provides a good estimate of the amount of pyrolysis products formed in the gas phase. To measure this quantity, the reactor assembly was attached to a pre-vacuumed stainless steel line with an internal diameter of 6.35 mm. The vacuum line was connected to a MKS 122A pressure gauge and a MKS PDR-0-1 digital
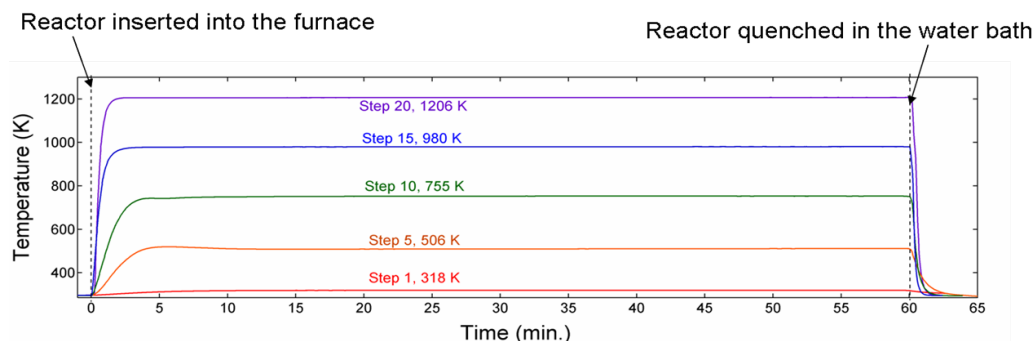
Figure 4: Measured sample temperature as a function of time for five different steps in the phenolic pyrolysis experiments.

readout for accurate pressure measurements. The needle valve of the reactor assembly was then opened, and the pressure reading was used to calculate the original reactor pressure based on the volumes of the reactor assembly (approximately 73 mL) and the vacuum line (approximately 32 mL). Between 650–1950 Pa (5–15 torr) of n-pentane vapor, which was used as an external standard for analyzing gaseous products, was then added to the reactor from a separate port connected to the vacuum line. The amount of n-pentane vapor added was determined by the additional pressure increase measured from the pressure gauge. The needle valve was then closed and the reactor assembly was taken for GC analysis.

Identification of pyrolysis products was performed by an Agilent 6890N GC system equipped with a 5975 mass selective detector (MSD) using preliminary pyrolysis results obtained prior to the step-wise experiments. For species quantification, the reactor assembly was attached to a 4.5 mL pre-vacuumed chamber with a sample extraction port that allows gas-tight syringes to extract samples. Once the reactor assembly and the vacuum cham-

9

ber were connected, the needle valve of the reactor assembly was opened to allow the sample to flow into the vacuum chamber before the valve was closed. A 2 mL gas phase sample was taken using a gas-tight syringe (Supelco) through the sample extraction port of the vacuum chamber. The sample was then immediately injected into an Agilent 7820A GC equipped with a thermal conductivity detector (TCD) and a Restek ShinCarbon ST 80/100 packed column (with an internal diameter of 2 mm and a length of 2 m) to quantify permanent gases. High purity helium (Airgas) with a constant flow pressure of 12 psi was used as the carrier gas in the column. The temperature of the inlet was set at 225 ^{o}C. The GC oven was programmed with the following temperature regime: hold at 35 ^{o}C for 2 min, ramp to 50 ^{o}C at 5 ^{o}C/min, hold at 50 ^{o}C for 3 min, ramp to 230 ^{o}C at 15 ^{o}C/min, and hold at 230 ^{o}C for 10 min. The detector temperature was set at 200 ^{o}C, with a reference gas flow rate of 15 mL/min and a makeup gas flow rate of 5 mL/min.

After the sample was injected, the reactor assembly was again connected to the vacuumed chamber. The same sample extraction procedure was repeated, except that a 1 mL gas phase sample was taken for an injection into the GC/MSD system equipped with a Restek Q-Bond PLOT column (with an internal diameter of 0.32 mm, a length of 30 m, and a film thickness of 10 μm) to quantify water vapor. The carrier gas (high purity helium) for this analysis was set at a constant flow rate of 3 mL/min. The temperature of the inlet was set at 250 ^{o}C. The GC oven was programmed with the following temperature regime: start at 35 ^{o}C, ramp to 50 ^{o}C at 15 ^{o}C/min, ramp to 100 ^{o}C at 5 ^{o}C/min, hold at 100 ^{o}C for 3 min, ramp to 250 ^{o}C at 25 ^{o}C/min,

162 and hold at 250 ^{o}C for 4 min.

163 The extraction procedure was repeated for the third time to extract a 1
164 mL gas phase sample for an injection into the Agilent 7820A GC equipped
165 with a flame ionization detector (FID) and a Restek Q-Bond PLOT column
166 to quantify light ($< C_9$) hydrocarbons. High purity helium carrier gas was
167 maintained at a constant pressure of 14.931 psi. The temperature of the
168 inlet was set at 250 ^{o}C. A split of the carrier gas (1:10) was used. The GC
169 oven was programmed with the following temperature regime: start at 35
170 ^{o}C, ramp to 50 ^{o}C at 15 ^{o}C/min, ramp to 100 ^{o}C at 5 ^{o}C/min, hold at 100
171 ^{o}C for 3 min, ramp to 250 ^{o}C at 25 ^{o}C/min, and hold at 250 ^{o}C for 4 min.
172 The FID temperature was set at 300 ^{o}C, with a hydrogen gas flow rate of 30
173 mL/min and a air flow rate of 400 mL/min.

174 After these gas phase GC analysis, the reactor assembly was disassembled.
175 The quartz reactor was capped to avoid penetration of ambient air humidity
176 into the sample. To quantify liquid phase products in the condenser, 15
177 mL of dichloromethane were used to rinse the stainless steel sections of the
178 reactor assembly. At the same time, 5–10 mg of biphenyl were added into
179 the solution as an external standard for the quantification of liquid products.
180 The solution was collected for further GC analysis using FID and a Restek
181 Rxi®-5Sil MS capillary column (with an internal diameter of 0.25 mm, a
182 length of 30 m, and a film thickness of 0.25 μm) to analyze aromatics and
183 aromatic alcohol (phenol derivatives) compounds. For this analysis, 5 μL of
184 the solution was injected, and the temperature of the GC inlet was set at 300
185 ^{o}C. The carrier gas was set at a constant pressure of 4.87 psi, with a split of
186 the carrier gas (high purity helium) at 1:10. The GC oven was programmed

187 with the following temperature regime: hold at 30 ^oC for 5 min, ramp to 180
188 ^oC at 7.5 ^oC/min, hold at 180 ^oC for 5 min, ramp to 285 ^oC at 15 ^oC/min,
189 and hold at 285 ^oC for 8 min.

190 The above GC analytical techniques allow detection and quantification of
191 any hydrocarbon or permanent gas species with a molecular weight smaller
192 than approximately 400 g/mol.

193 Lastly, an electronic balance (Ohaus AV264C) with a repeatability of
194 0.1 mg was used to measure the weight of the capped quartz reactor for
195 the determination of mass loss after each 50 K increment. The stainless
196 steel reactor assembly was cleaned with dichloromethane and then dried in
197 a convection oven at 373 K for 30 minutes before being reassembled for the
198 next run. This elementary procedure was then repeated using the same
199 sample, with the furnace temperature set at 50 K higher than the previous
200 run. The first experiment in this step-wise procedure started with a furnace
201 temperature of 323 K, and the procedure was repeated with 50 K increments
202 until a furnace temperature of 1373 K.

203 In this work, three sets of phenolic pyrolysis experiments with an identical
204 step-wise procedure were performed to confirm reproducibility. Standard
205 deviations of the three experiment sets were used as error bars in our figures.

206 **3. Results and discussion**

207 *3.1. GC Calibration*

208 GC calibration for each of the analytical techniques was performed by
209 analysis of reference chemical standards, which allowed response factors for
210 any detectable species to be calculated. Linear responses were obtained in

211   each case. The response factors were used to quantify H_2, CO, CH_4, CO_2,

212   C_2H_4, and C_2H_6 using GC/TCD, H_2O using GC/MSD, and all hydrocarbon

213   compounds using GC/FID. Details of how GC calibrations were performed

214   and how response factors were obtained are provided in the Supplemental

215   Information section.

216   *3.2. Reaction temperature, mass yields, and pressure*

217   Figure 5 shows measured sample temperature against furnace set temper-

218   ature during the pyrolysis experiments. The ferrule temperature, which is

219   the temperature at the interface between the quartz reactor and the stainless

220   steel assembly, was also measured and plotted in the figure. As illustrated

221   in the figure, measured sample temperatures are linearly dependent on the

222   furnace set temperature, but usually lower by between 3–80 K, depending on

223   the set temperature. The ferrule temperature never exceeded 450 K, which

224   suggests that the temperature gradient above the sample is large and any

225   homogeneous gas phase chemistry above the pyrolysis zone is significantly

226   quenched due to low headspace temperatures.

227   The mass yields quantified by GC are plotted in Figure 6 against mass

228   loss measured by the electronic balance. As shown in the figure, the mass

229   loss of the phenol-formaldehyde resin peaks at 750 K. According to our GC

230   analysis, water is the dominant product below 800 K. As the reaction temper-

231   ature increases, liquid products extracted from the dichloromethane solution,

232   containing mostly aromatics and aromatic alcohols, start to form in a tem-

233   perature range between 500 and 850 K. Above 800 K, permanent gases are

234   the major products. Figure 6 also shows that at lower temperatures, the mass

235   yields from the GC measurements were lower than the mass loss measured
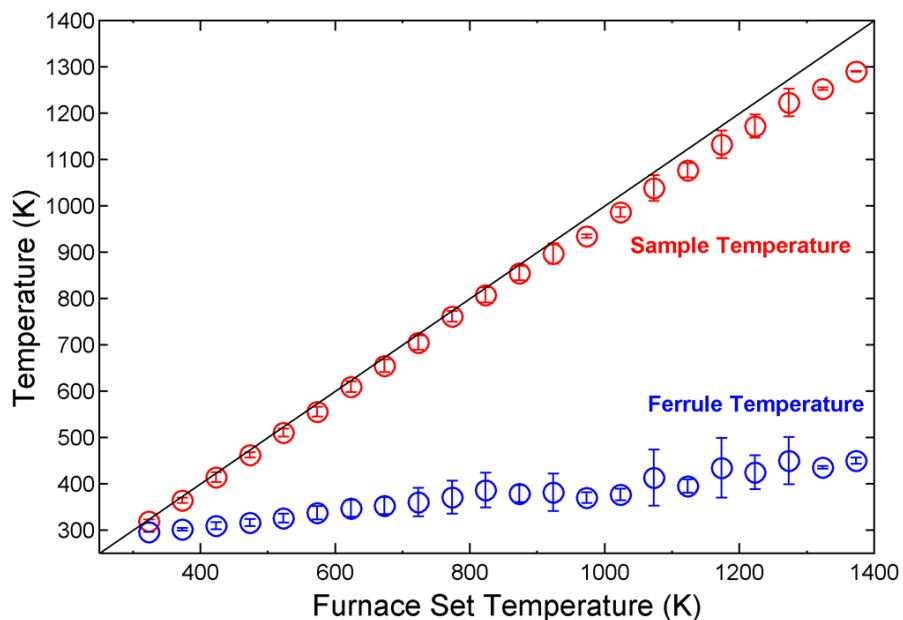
Figure 5: Comparison of measured sample and ferrule temperatures against furnace set temperature in the phenolic pyrolysis experiments.

from the balance. This is because water is the most dominant species in this temperature range, and water quantification using GC is subject to large errors due to exposure to ambient humidity throughout the analytical process. At higher temperatures, mass loss is very minor, and it is challenging for the electronic balance to accurately determine such a small mass difference, resulting in mass yields from the GC measurements higher than the mass loss measured from the balance. In general, however, the agreement between the two measurements is good, within 0.5 mg. The accumulated mass loss as a function of reaction temperature, derived from Figure 6, is shown in Figure 7. As illustrated in the figure, 39.2% of the initial sample mass is lost by pyrolysis after a reaction temperature of 1290 K.
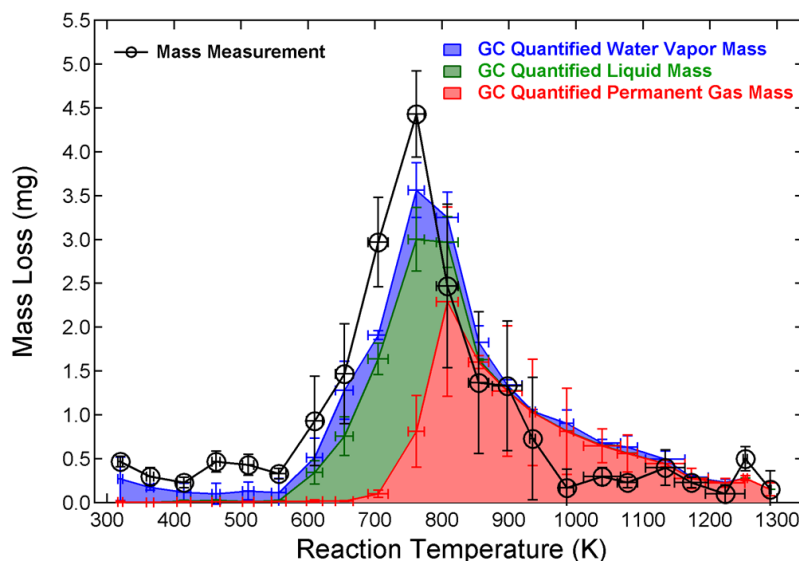
14

Figure 6: The mass yields as a function of temperature from the phenolic pyrolysis experiments.

247   A validation of the stepwise mass loss measurements was performed by
248 thermo-gravimetric analysis (TGA). We used a commercial TGA system
249 (Thermal Analyzer STA 449 F3 Jupiter, Netzsch, Burlington, MA) to test a
250 sample of approximately 4 g, at temperatures up to 1670 K. The measure-
251 ment was performed at a heating rate of 10 K/min in inert atmosphere. The
252 chamber was evacuated to a base pressure of 10^{-2} Pa and filled with Ar gas
253 up to room atmosphere. During the heating phase a constant flow of Ar
254 at 200 ml/min was supplied, preventing the infiltration of external oxidants
255 and providing adequate flushing of the pyrolysis gases. The instrument was
256 calibrated prior to the test under the same operating conditions.
257   The measured mass loss obtained from TGA is plotted in Figure 8 against
258 the mass loss measurements obtained from the laboratory experiments (with
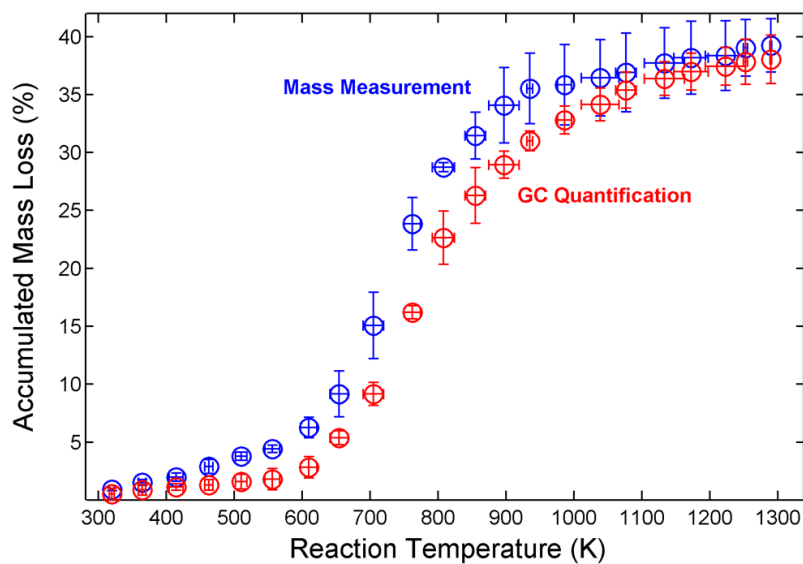
Figure 7: The accumulated mass yields from the phenolic pyrolysis experiments.

the electronic balance and gas chromatography, respectively). As illustrated in the figure, all three mass loss measurements are agreeable.

The reactor pressure measured at room temperature after each pyrolysis step is shown in Figure 9. As illustrated in the figure, the final reactor pressure peaked at a pyrolysis temperature of 900 K and dropped afterwards. The increase and drop in this pressure did not exactly follow the mass loss trend in Figure 6: pressure plot peaked at a higher temperature (900 K) than the mass loss plot (750 K) did. This suggests that at a reaction temperature near 900 K, similar or even less amount (in terms of mass) of sample is pyrolyzed, but smaller species, such as hydrogen gas, is formed, resulting in higher molar yields and thus higher system pressure.
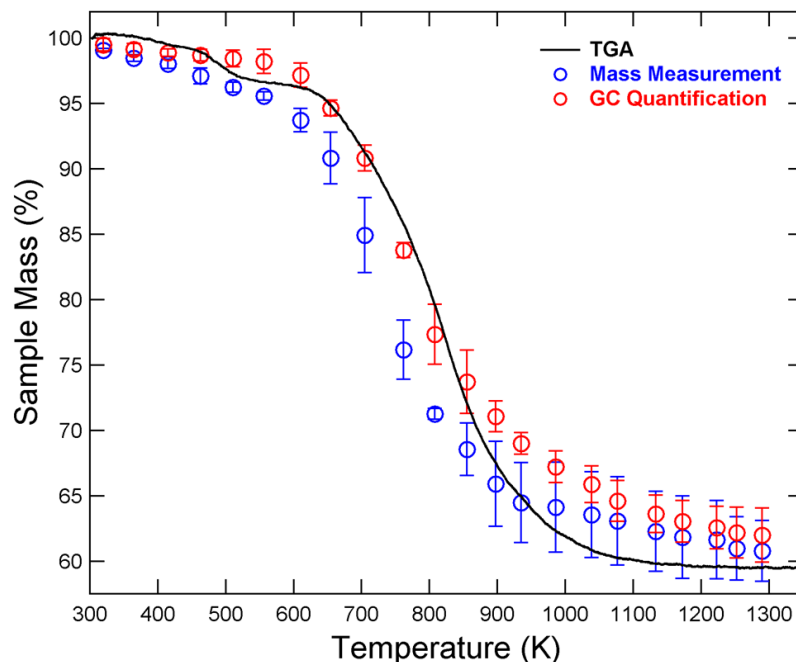
Figure 8: The accumulated mass yields from the phenolic pyrolysis experiments.

3.3. Species yields

In this study, four different families of pyrolysis products were identified by GC analysis. A representative chromatograph for the 855 K decomposition step is shown in Figure 10. These families of products include (1) water vapor and permanent gases, such as hydrogen (H_2), carbon monoxide (CO), carbon dioxide (CO_2), methane (CH_4); (2) light hydrocarbons, such as ethene (C_2H_4), ethane (C_2H_6), propene (C_3H_6), propane (C_3H_8), butene (C_4H_8), and butane (C_4H_{10}); (3) aromatics, such as benzene (C_6H_6), toluene (C_7H_8), and xylene (C_8H_{10}); (4) aromatic alcohols (phenol derivatives), such as phenol (C_6H_6O), cresol (C_7H_8O), xylenol (dimethylphenol, $C_8H_{10}O$), and trimethylphenol ($C_9H_{12}O$). All identified products are consistent with previ-

17
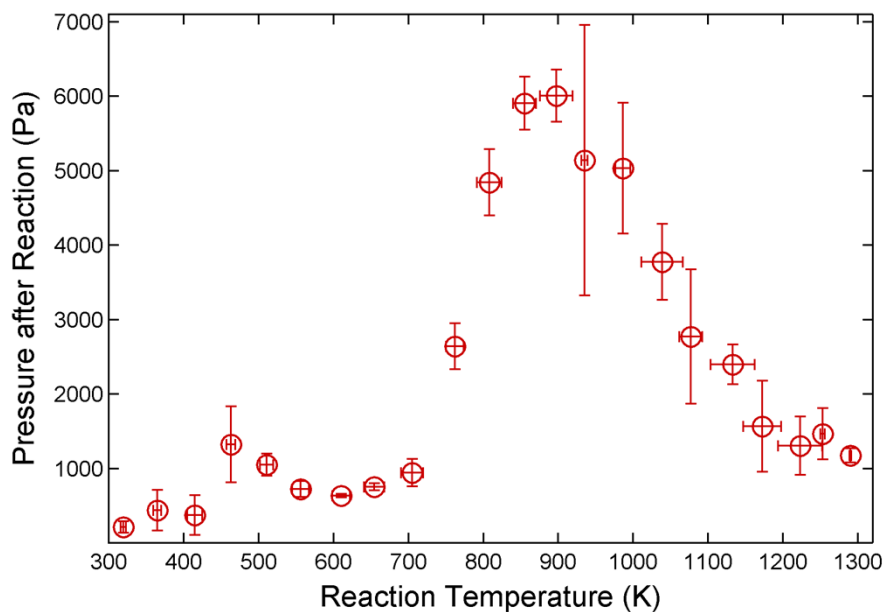
Figure 9: The final pressure measured at room temperature after each run as a function of reaction temperature.

281 ous experimental findings by Sykes and Trick et al. [1, 2, 21].

282 The molar and mass yields of pyrolysis products at each pyrolysis tem-
283 perature are summarized and tabulated in Tables 1 and 2. The temperature
284 dependent product yields are also plotted in Figures 11 to 14. As illustrated
285 in Figure 11, water vapor is the main product at low temperatures (< 800 K),
286 and permanent gases, including hydrogen, methane, CO, and CO_2, become
287 more dominant at higher (> 800 K) temperatures. Hydrogen gas is the most
288 abundant product at temperatures above 900 K, and its molar yields account
289 for most of the pressure increase at high pyrolysis temperatures (as shown in
290 Figure 9). In addition to permanent gases, light hydrocarbons, such as C_2 to
291 C_4 hydrocarbons, are also produced from phenolic resin pyrolysis, as shown

18
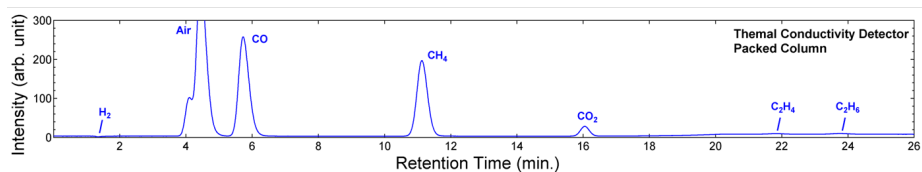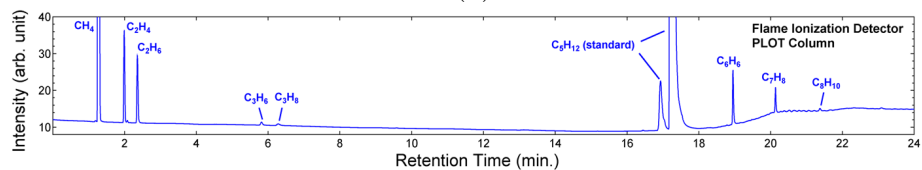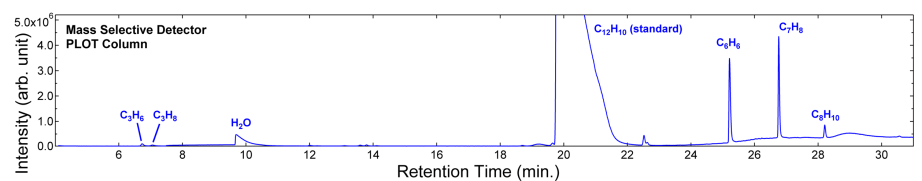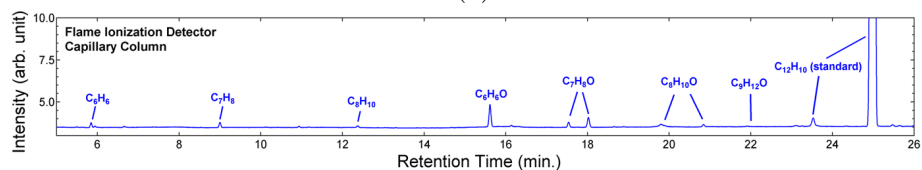
Figure 10: A chromatograph from our gas chromatography (GC) analysis using (a) packed column with TCD, (b) PLOT column with FID, (c) PLOT column with MSD, and (d) capillary column with FID. The reaction temperature was 855 K.

in Figure 12. Interestingly, the yields of these species dramatically increase at temperatures above 800 K and then drop after 1000 K. Their yields are low compared to permanent gases. The production of these hydrocarbons were not reported in Sykes' experiments, and they may be formed via radical

296 recombination reactions in the colder zones of the reactor headspace. The
297 yields of aromatic species are shown in Figure 13. Their yields are only signif-
298 icant at reaction temperatures between 700 and 850 K, which are comparable
299 with yields of light hydrocarbons except ethane. At a reaction temperature
300 above 850 K, the yields of these aromatic products become negligible. Fi-
301 nally, phenol and its derivatives, as shown in Figure 14, are significant in a
302 temperature range between 500 and 850 K. Among them, phenol and cresol
303 have the highest yields.
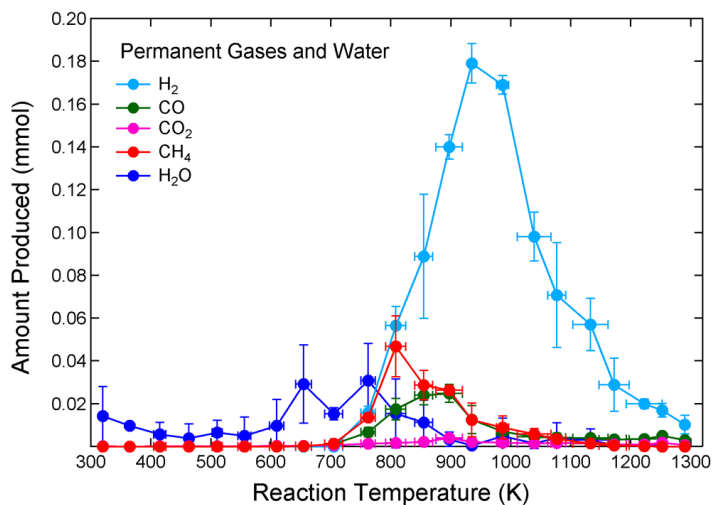
Figure 11: The amount of permanent gases produced from phenolic pyrolysis as a function of reaction (sample) temperature.
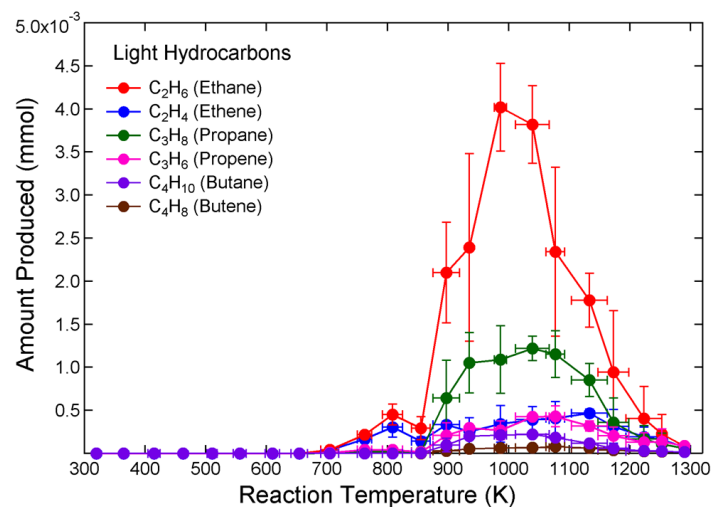
Figure 12: The amount of light hydrocarbons produced from phenolic pyrolysis as a function of reaction (sample) temperature.

Figure 13: The amount of aromatic compounds produced from phenolic pyrolysis as a function of reaction (sample) temperature.

Figure 14: The amount of aromatic alcohols produced from phenolic pyrolysis as a function of reaction (sample) temperature.

22

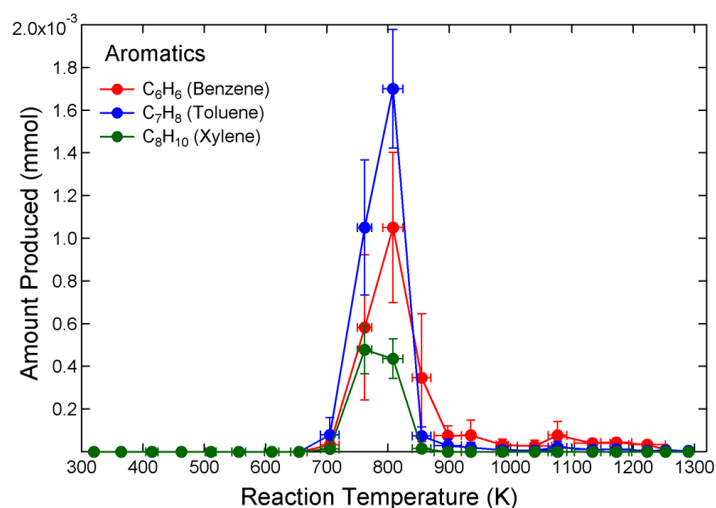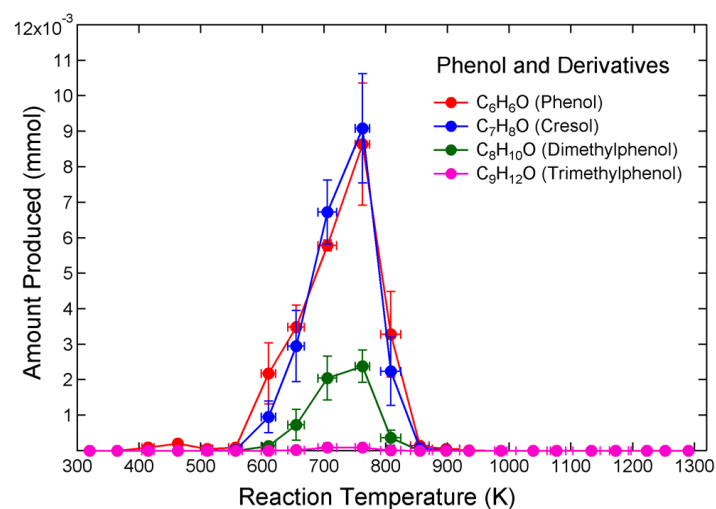| Pyrolysis temperature (K)	Molar yields (mmol)						
	H_2O	H_2	CH_4	CO	CO_2	C_2H_4	C_2H_6
320	$1.42 \cdot 10^{-2}$				$8.63 \cdot 10^{-3}$		
364	$9.64 \cdot 10^{-3}$				$2.83 \cdot 10^{-3}$		
415	$5.66 \cdot 10^{-3}$				$8.27 \cdot 10^{-3}$		
463	$3.84 \cdot 10^{-3}$		$1.63 \cdot 10^{-5}$	$3.16 \cdot 10^{-5}$	$7.45 \cdot 10^{-3}$		
511	$6.53 \cdot 10^{-3}$		$1.55 \cdot 10^{-5}$	$1.69 \cdot 10^{-4}$	$3.77 \cdot 10^{-3}$		
556	$4.99 \cdot 10^{-3}$		$2.55 \cdot 10^{-5}$	$1.47 \cdot 10^{-4}$	$7.63 \cdot 10^{-3}$		
610	$9.64 \cdot 10^{-3}$		$7.18 \cdot 10^{-5}$	$9.22 \cdot 10^{-5}$	$1.67 \cdot 10^{-2}$		
654	$2.91 \cdot 10^{-2}$		$1.26 \cdot 10^{-4}$	$1.45 \cdot 10^{-4}$	$1.24 \cdot 10^{-2}$		
705	$1.52 \cdot 10^{-2}$		$1.28 \cdot 10^{-3}$	$1.18 \cdot 10^{-3}$	$2.84 \cdot 10^{-2}$	$3.89 \cdot 10^{-5}$	$3.99 \cdot 10^{-5}$
762	$3.08 \cdot 10^{-2}$	$1.58 \cdot 10^{-2}$	$1.36 \cdot 10^{-2}$	$6.65 \cdot 10^{-3}$	$6.10 \cdot 10^{-2}$	$1.67 \cdot 10^{-4}$	$2.19 \cdot 10^{-4}$
808	$1.55 \cdot 10^{-2}$	$5.65 \cdot 10^{-2}$	$4.68 \cdot 10^{-2}$	$1.75 \cdot 10^{-2}$	$7.61 \cdot 10^{-2}$	$3.04 \cdot 10^{-4}$	$4.51 \cdot 10^{-4}$
855	$1.13 \cdot 10^{-2}$	$8.89 \cdot 10^{-2}$	$2.86 \cdot 10^{-2}$	$2.39 \cdot 10^{-2}$	$9.29 \cdot 10^{-2}$	$1.40 \cdot 10^{-4}$	$2.93 \cdot 10^{-4}$
897	$3.28 \cdot 10^{-3}$	$1.40 \cdot 10^{-1}$	$2.64 \cdot 10^{-2}$	$2.48 \cdot 10^{-2}$	$1.80 \cdot 10^{-1}$	$3.34 \cdot 10^{-4}$	$2.10 \cdot 10^{-3}$
935	$5.65 \cdot 10^{-4}$	$1.79 \cdot 10^{-1}$	$1.24 \cdot 10^{-2}$	$1.25 \cdot 10^{-2}$	$9.90 \cdot 10^{-2}$	$2.54 \cdot 10^{-4}$	$2.39 \cdot 10^{-3}$
986	$4.79 \cdot 10^{-3}$	$1.69 \cdot 10^{-1}$	$8.93 \cdot 10^{-3}$	$7.03 \cdot 10^{-3}$	$7.77 \cdot 10^{-2}$	$3.44 \cdot 10^{-4}$	$4.02 \cdot 10^{-3}$
1039	$1.44 \cdot 10^{-3}$	$9.80 \cdot 10^{-2}$	$5.89 \cdot 10^{-3}$	$4.50 \cdot 10^{-3}$	$6.30 \cdot 10^{-2}$	$3.92 \cdot 10^{-4}$	$3.82 \cdot 10^{-3}$
1077	$4.09 \cdot 10^{-3}$	$7.08 \cdot 10^{-2}$	$3.46 \cdot 10^{-3}$	$4.13 \cdot 10^{-3}$	$7.51 \cdot 10^{-2}$	$4.09 \cdot 10^{-4}$	$2.34 \cdot 10^{-3}$
1133	$2.97 \cdot 10^{-3}$	$5.70 \cdot 10^{-2}$	$1.55 \cdot 10^{-3}$	$3.94 \cdot 10^{-3}$	$6.40 \cdot 10^{-2}$	$4.66 \cdot 10^{-4}$	$1.78 \cdot 10^{-3}$
1173	$6.76 \cdot 10^{-4}$	$2.89 \cdot 10^{-2}$	$4.84 \cdot 10^{-4}$	$3.37 \cdot 10^{-3}$	$4.55 \cdot 10^{-2}$	$3.14 \cdot 10^{-4}$	$9.43 \cdot 10^{-4}$
1223	$8.30 \cdot 10^{-4}$	$2.00 \cdot 10^{-2}$	$1.36 \cdot 10^{-4}$	$3.55 \cdot 10^{-3}$	$4.62 \cdot 10^{-2}$	$1.91 \cdot 10^{-4}$	$4.05 \cdot 10^{-4}$
1253		$1.70 \cdot 10^{-2}$	$5.11 \cdot 10^{-5}$	$5.02 \cdot 10^{-3}$	$7.95 \cdot 10^{-2}$	$1.57 \cdot 10^{-4}$	$2.24 \cdot 10^{-4}$
1290		$1.03 \cdot 10^{-2}$	$3.25 \cdot 10^{-5}$	$3.00 \cdot 10^{-3}$	$7.12 \cdot 10^{-4}$	$7.70 \cdot 10^{-5}$	$8.23 \cdot 10^{-5}$
Total	$1.75 \cdot 10^{-1}$	$9.51 \cdot 10^{-1}$	$1.50 \cdot 10^{-1}$	$1.22 \cdot 10^{-1}$	$2.47 \cdot 10^{-2}$	$3.59 \cdot 10^{-3}$	$1.91 \cdot 10^{-2}$

Pyrolysis temperature (K)	Molar yields (mmol)						
	C_3H_6	C_3H_8	C_4H_8	C_4H_{10}	C_6H_6	C_7H_8	C_8H_{10}
320							
364							
415							
463							
511							
556							
610							
654							
705	$9.65 \cdot 10^{-6}$	$3.73 \cdot 10^{-6}$			$3.15 \cdot 10^{-5}$	$7.96 \cdot 10^{-5}$	$1.42 \cdot 10^{-5}$
762	$4.33 \cdot 10^{-5}$	$1.90 \cdot 10^{-5}$			$5.83 \cdot 10^{-4}$	$1.05 \cdot 10^{-3}$	$4.78 \cdot 10^{-4}$
808	$4.16 \cdot 10^{-5}$	$2.17 \cdot 10^{-5}$			$1.05 \cdot 10^{-3}$	$1.70 \cdot 10^{-3}$	$4.36 \cdot 10^{-4}$
855	$1.62 \cdot 10^{-5}$	$2.12 \cdot 10^{-5}$		$5.54 \cdot 10^{-6}$	$3.46 \cdot 10^{-4}$	$7.47 \cdot 10^{-5}$	$1.52 \cdot 10^{-5}$
897	$2.09 \cdot 10^{-4}$	$6.42 \cdot 10^{-4}$	$2.85 \cdot 10^{-5}$	$9.72 \cdot 10^{-5}$	$7.61 \cdot 10^{-5}$	$2.86 \cdot 10^{-5}$	
935	$2.96 \cdot 10^{-4}$	$1.05 \cdot 10^{-3}$	$5.62 \cdot 10^{-5}$	$2.02 \cdot 10^{-4}$	$7.78 \cdot 10^{-5}$	$2.10 \cdot 10^{-5}$	
986	$2.68 \cdot 10^{-4}$	$1.09 \cdot 10^{-3}$	$6.34 \cdot 10^{-5}$	$2.12 \cdot 10^{-4}$	$3.14 \cdot 10^{-5}$	$7.73 \cdot 10^{-6}$	
1039	$4.27 \cdot 10^{-4}$	$1.22 \cdot 10^{-3}$	$6.62 \cdot 10^{-5}$	$2.21 \cdot 10^{-4}$	$2.67 \cdot 10^{-5}$	$7.31 \cdot 10^{-6}$	
1077	$4.31 \cdot 10^{-4}$	$1.15 \cdot 10^{-3}$	$7.76 \cdot 10^{-5}$	$1.85 \cdot 10^{-4}$	$7.79 \cdot 10^{-5}$	$2.25 \cdot 10^{-5}$	
1133	$3.19 \cdot 10^{-4}$	$8.52 \cdot 10^{-4}$	$6.39 \cdot 10^{-5}$	$1.16 \cdot 10^{-4}$	$4.06 \cdot 10^{-5}$	$1.01 \cdot 10^{-5}$	
1173	$2.06 \cdot 10^{-4}$	$3.60 \cdot 10^{-4}$	$3.64 \cdot 10^{-5}$	$5.91 \cdot 10^{-5}$	$4.44 \cdot 10^{-5}$	$1.10 \cdot 10^{-5}$	
1223	$1.30 \cdot 10^{-4}$	$1.68 \cdot 10^{-4}$	$2.56 \cdot 10^{-5}$	$3.09 \cdot 10^{-5}$	$3.36 \cdot 10^{-5}$	$5.36 \cdot 10^{-6}$	
1253	$1.39 \cdot 10^{-4}$	$1.09 \cdot 10^{-4}$	$1.92 \cdot 10^{-5}$	$2.60 \cdot 10^{-5}$	$9.40 \cdot 10^{-6}$	$7.16 \cdot 10^{-6}$	
1290	$8.84 \cdot 10^{-5}$	$5.84 \cdot 10^{-5}$	$1.47 \cdot 10^{-5}$	$1.49 \cdot 10^{-5}$	$3.56 \cdot 10^{-6}$	$4.73 \cdot 10^{-6}$	
Total	$2.62 \cdot 10^{-3}$	$6.76 \cdot 10^{-3}$	$4.52 \cdot 10^{-4}$	$1.17 \cdot 10^{-3}$	$2.43 \cdot 10^{-3}$	$3.02 \cdot 10^{-3}$	$9.43 \cdot 10^{-4}$

Pyrolysis temperature (K)	Molar yields (mmol)			
	C_6H_6O	C_7H_8O	$C_8H_{10}O$	$C_9H_{12}O$
320				
364				
415	$9.25 \cdot 10^{-5}$			
463	$1.98 \cdot 10^{-4}$			
511	$4.93 \cdot 10^{-5}$			
556	$9.52 \cdot 10^{-5}$	$2.52 \cdot 10^{-5}$		
610	$2.18 \cdot 10^{-3}$	$9.56 \cdot 10^{-4}$	$1.31 \cdot 10^{-4}$	
654	$3.48 \cdot 10^{-3}$	$2.95 \cdot 10^{-3}$	$7.25 \cdot 10^{-4}$	$2.51 \cdot 10^{-5}$
705	$5.78 \cdot 10^{-3}$	$6.72 \cdot 10^{-3}$	$2.05 \cdot 10^{-3}$	$8.98 \cdot 10^{-5}$
762	$8.64 \cdot 10^{-3}$	$9.08 \cdot 10^{-3}$	$2.38 \cdot 10^{-3}$	$9.13 \cdot 10^{-5}$
808	$3.28 \cdot 10^{-3}$	$2.24 \cdot 10^{-3}$	$3.66 \cdot 10^{-4}$	$7.71 \cdot 10^{-6}$
855	$1.39 \cdot 10^{-4}$	$6.73 \cdot 10^{-5}$		
897	$4.84 \cdot 10^{-5}$	$6.99 \cdot 10^{-6}$		
935	$1.45 \cdot 10^{-5}$			
986	$2.84 \cdot 10^{-6}$			
1039				
1077				
1133				
1173				
1223				
1253				
1290				
Total	$2.40 \cdot 10^{-2}$	$2.21 \cdot 10^{-2}$	$5.66 \cdot 10^{-3}$	$2.14 \cdot 10^{-4}$

Table 1: Molar yields of pyrolysis products versus pyrolysis temperature.

Pyrolysis	Mass yields (mg)						
temperature (K)	H_2O	H_2	CH_4	CO	CO_2	C_2H_4	C_2H_6
320	$2.57 \cdot 10^{-1}$				$8.63 \cdot 10^{-3}$		
364	$1.74 \cdot 10^{-1}$				$2.83 \cdot 10^{-3}$		
415	$1.02 \cdot 10^{-1}$				$8.27 \cdot 10^{-3}$		
463	$6.92 \cdot 10^{-2}$		$2.62 \cdot 10^{-4}$	$8.86 \cdot 10^{-4}$	$7.45 \cdot 10^{-3}$		
511	$1.18 \cdot 10^{-1}$		$2.48 \cdot 10^{-4}$	$4.74 \cdot 10^{-3}$	$3.77 \cdot 10^{-3}$		
556	$8.99 \cdot 10^{-2}$		$4.10 \cdot 10^{-4}$	$4.12 \cdot 10^{-3}$	$7.63 \cdot 10^{-3}$		
610	$1.74 \cdot 10^{-1}$		$1.15 \cdot 10^{-3}$	$2.58 \cdot 10^{-3}$	$1.67 \cdot 10^{-2}$		
654	$5.24 \cdot 10^{-1}$		$2.03 \cdot 10^{-3}$	$4.07 \cdot 10^{-3}$	$1.24 \cdot 10^{-2}$		
705	$2.74 \cdot 10^{-1}$		$2.05 \cdot 10^{-2}$	$3.30 \cdot 10^{-2}$	$2.84 \cdot 10^{-2}$	$1.09 \cdot 10^{-3}$	$1.20 \cdot 10^{-3}$
762	$5.55 \cdot 10^{-1}$	$3.18 \cdot 10^{-2}$	$2.18 \cdot 10^{-1}$	$1.86 \cdot 10^{-1}$	$6.10 \cdot 10^{-2}$	$4.68 \cdot 10^{-3}$	$6.59 \cdot 10^{-3}$
808	$2.78 \cdot 10^{-1}$	$1.14 \cdot 10^{-1}$	$7.51 \cdot 10^{-1}$	$4.90 \cdot 10^{-1}$	$7.61 \cdot 10^{-2}$	$8.53 \cdot 10^{-3}$	$1.36 \cdot 10^{-2}$
855	$2.04 \cdot 10^{-1}$	$1.79 \cdot 10^{-1}$	$4.58 \cdot 10^{-1}$	$6.70 \cdot 10^{-1}$	$9.29 \cdot 10^{-2}$	$3.93 \cdot 10^{-3}$	$8.81 \cdot 10^{-3}$
897	$5.91 \cdot 10^{-2}$	$2.82 \cdot 10^{-1}$	$4.24 \cdot 10^{-1}$	$6.94 \cdot 10^{-1}$	$1.80 \cdot 10^{-1}$	$9.37 \cdot 10^{-3}$	$6.32 \cdot 10^{-2}$
935	$1.02 \cdot 10^{-2}$	$3.60 \cdot 10^{-1}$	$2.00 \cdot 10^{-1}$	$3.50 \cdot 10^{-1}$	$9.90 \cdot 10^{-2}$	$7.12 \cdot 10^{-3}$	$7.17 \cdot 10^{-2}$
986	$8.63 \cdot 10^{-2}$	$3.41 \cdot 10^{-1}$	$1.43 \cdot 10^{-1}$	$1.97 \cdot 10^{-1}$	$7.77 \cdot 10^{-2}$	$9.64 \cdot 10^{-3}$	$1.21 \cdot 10^{-1}$
1039	$2.60 \cdot 10^{-2}$	$1.98 \cdot 10^{-1}$	$9.45 \cdot 10^{-2}$	$1.26 \cdot 10^{-1}$	$6.30 \cdot 10^{-2}$	$1.10 \cdot 10^{-2}$	$1.15 \cdot 10^{-1}$
1077	$7.36 \cdot 10^{-2}$	$1.43 \cdot 10^{-1}$	$5.54 \cdot 10^{-2}$	$1.16 \cdot 10^{-1}$	$7.51 \cdot 10^{-2}$	$1.15 \cdot 10^{-2}$	$7.04 \cdot 10^{-2}$
1133	$5.35 \cdot 10^{-2}$	$1.15 \cdot 10^{-1}$	$2.48 \cdot 10^{-2}$	$1.10 \cdot 10^{-1}$	$6.41 \cdot 10^{-2}$	$1.31 \cdot 10^{-2}$	$5.34 \cdot 10^{-2}$
1173	$1.22 \cdot 10^{-2}$	$5.84 \cdot 10^{-2}$	$7.77 \cdot 10^{-3}$	$9.43 \cdot 10^{-2}$	$4.55 \cdot 10^{-2}$	$8.81 \cdot 10^{-3}$	$2.84 \cdot 10^{-2}$
1223	$1.50 \cdot 10^{-2}$	$4.02 \cdot 10^{-2}$	$2.18 \cdot 10^{-3}$	$9.95 \cdot 10^{-2}$	$4.62 \cdot 10^{-2}$	$5.37 \cdot 10^{-3}$	$1.22 \cdot 10^{-2}$
1253		$3.43 \cdot 10^{-2}$	$8.21 \cdot 10^{-4}$	$1.41 \cdot 10^{-1}$	$7.95 \cdot 10^{-2}$	$4.41 \cdot 10^{-3}$	$6.74 \cdot 10^{-3}$
1290		$2.07 \cdot 10^{-2}$	$5.21 \cdot 10^{-4}$	$8.41 \cdot 10^{-2}$	$3.14 \cdot 10^{-2}$	$2.16 \cdot 10^{-3}$	$2.47 \cdot 10^{-3}$
Total	3.153	1.917	2.404	3.408	1.087	0.101	0.574

Pyrolysis	Mass yields (mg)						
temperature (K)	C_3H_6	C_3H_8	C_4H_8	C_4H_{10}	C_6H_6	C_7H_8	C_8H_{10}
320							
364							
415							
463							
511							
556							
610							
654							
705	$4.06 \cdot 10^{-4}$	$1.65 \cdot 10^{-4}$			$2.46 \cdot 10^{-3}$	$7.33 \cdot 10^{-3}$	$1.51 \cdot 10^{-3}$
762	$1.82 \cdot 10^{-3}$	$8.37 \cdot 10^{-4}$			$4.56 \cdot 10^{-2}$	$9.63 \cdot 10^{-2}$	$5.07 \cdot 10^{-2}$
808	$1.75 \cdot 10^{-3}$	$9.58 \cdot 10^{-4}$			$8.21 \cdot 10^{-2}$	$1.56 \cdot 10^{-1}$	$4.63 \cdot 10^{-2}$
855	$6.83 \cdot 10^{-4}$	$9.34 \cdot 10^{-4}$		$3.22 \cdot 10^{-4}$	$2.70 \cdot 10^{-2}$	$6.88 \cdot 10^{-3}$	$1.61 \cdot 10^{-3}$
897	$8.80 \cdot 10^{-3}$	$2.83 \cdot 10^{-2}$	$1.60 \cdot 10^{-3}$	$5.65 \cdot 10^{-3}$	$5.94 \cdot 10^{-3}$	$2.63 \cdot 10^{-3}$	
935	$1.25 \cdot 10^{-2}$	$4.63 \cdot 10^{-2}$	$3.15 \cdot 10^{-3}$	$1.17 \cdot 10^{-2}$	$6.08 \cdot 10^{-3}$	$1.94 \cdot 10^{-3}$	
986	$1.13 \cdot 10^{-2}$	$4.79 \cdot 10^{-2}$	$3.56 \cdot 10^{-3}$	$1.23 \cdot 10^{-2}$	$2.45 \cdot 10^{-3}$	$7.12 \cdot 10^{-4}$	
1039	$1.80 \cdot 10^{-2}$	$5.37 \cdot 10^{-2}$	$3.71 \cdot 10^{-3}$	$1.29 \cdot 10^{-2}$	$2.09 \cdot 10^{-3}$	$6.73 \cdot 10^{-4}$	
1077	$1.82 \cdot 10^{-2}$	$5.08 \cdot 10^{-2}$	$4.36 \cdot 10^{-3}$	$1.08 \cdot 10^{-2}$	$6.08 \cdot 10^{-3}$	$2.08 \cdot 10^{-3}$	
1133	$1.34 \cdot 10^{-2}$	$3.76 \cdot 10^{-2}$	$3.59 \cdot 10^{-3}$	$6.73 \cdot 10^{-3}$	$3.17 \cdot 10^{-3}$	$9.34 \cdot 10^{-4}$	
1173	$8.65 \cdot 10^{-2}$	$1.59 \cdot 10^{-2}$	$2.04 \cdot 10^{-3}$	$3.44 \cdot 10^{-3}$	$3.47 \cdot 10^{-3}$	$1.01 \cdot 10^{-3}$	
1223	$5.49 \cdot 10^{-3}$	$7.40 \cdot 10^{-3}$	$1.44 \cdot 10^{-3}$	$1.79 \cdot 10^{-3}$	$2.62 \cdot 10^{-3}$	$4.97 \cdot 10^{-4}$	
1253	$5.85 \cdot 10^{-3}$	$4.81 \cdot 10^{-3}$	$1.08 \cdot 10^{-3}$	$1.51 \cdot 10^{-3}$	$7.34 \cdot 10^{-4}$	$6.60 \cdot 10^{-4}$	
1290	$3.72 \cdot 10^{-3}$	$2.58 \cdot 10^{-3}$	$8.26 \cdot 10^{-4}$	$8.64 \cdot 10^{-4}$	$2.78 \cdot 10^{-4}$	$4.36 \cdot 10^{-4}$	
Total	0.110	0.298	0.025	0.068	0.190	0.279	0.100

Pyrolysis temperature (K)	Mass yields (mg)			
	C_6H_6O	C_7H_8O	$C_8H_{10}O$	$C_9H_{12}O$
320				
364				
415	$8.70 \cdot 10^{-3}$			
463	$1.86 \cdot 10^{-2}$			
511	$4.64 \cdot 10^{-3}$			
556	$8.96 \cdot 10^{-3}$	$2.73 \cdot 10^{-3}$		
610	$2.05 \cdot 10^{-1}$	$1.03 \cdot 10^{-1}$	$1.60 \cdot 10^{-2}$	
654	$3.27 \cdot 10^{-1}$	$3.19 \cdot 10^{-1}$	$8.85 \cdot 10^{-2}$	$3.41 \cdot 10^{-3}$
705	$5.44 \cdot 10^{-1}$	$7.27 \cdot 10^{-1}$	$2.51 \cdot 10^{-1}$	$1.22 \cdot 10^{-2}$
762	$8.13 \cdot 10^{-1}$	$9.82 \cdot 10^{-1}$	$2.91 \cdot 10^{-1}$	$1.24 \cdot 10^{-2}$
808	$3.09 \cdot 10^{-1}$	$2.42 \cdot 10^{-1}$	$4.47 \cdot 10^{-2}$	$1.05 \cdot 10^{-3}$
855	$1.31 \cdot 10^{-2}$	$7.28 \cdot 10^{-3}$		
897	$4.55 \cdot 10^{-3}$	$7.56 \cdot 10^{-4}$		
935	$1.36 \cdot 10^{-3}$			
986	$2.67 \cdot 10^{-4}$			
1039				
1077				
1133				
1173				
1223				
1253				
1290				
Total	2.258	2.384	0.691	0.029

Table 2: Mass yields of pyrolysis products versus pyrolysis temperature.

4. Conclusion

A batch reactor system was designed and built specifically for this study to fully collect and quantitatively analyze products from phenol-formaldehyde resin pyrolysis. The experimental protocol was based on a step-wise heating procedure in a 50 K increment to pyrolyze a 50 mg sample from 320 to 1290 K. The pyrolysis products were identified and quantified using gas chromatography techniques. Key conclusions from our experiments are:

- The overall mass loss during a commercial resole type phenol-formaldehyde resin pyrolysis is 39.2% after a reaction temperature of 1290 K;

- Water is the most dominant pyrolysis product below a pyrolysis temperature of 800 K;

- Phenol derivatives (aromatic alcohols) are significant at a pyrolysis temperature between 500 and 850 K;

- Yields of aromatic products, including benzene, toluene, and xylene, are only significant between 700 and 850 K;

- Permanent gases such as hydrogen, methane, carbon monoxide, and carbon dioxide are mostly produced between 800 K and 1200 K;

- The yields of light hydrocarbons peak at 1000 K, although their yields are very minor compared to permanent gases.

Our results are consistent with available experimental findings and the widely accepted three stage pyrolysis mechanism. However, our work provides more quantitative details than previous experiments, which can be fur-

326 ther used to develop a more comprehensive chemical kinetic model deducing
327 detailed reaction pathways of phenol-formaldehyde resin pyrolysis.

336 References

337 [1] K. A. Trick, T. E. Saliba, Mechanisms of the pyrolysis of phenolic resin
338   in a carbon/phenolic composite, Carbon 33 (11) (1995) 1509–1515.

339 [2] K. A. Trick, T. E. Saliba, S. S. Sandhu, A kinetic model of the pyrolysis
340   of phenolic resin in a carbon/phenolic composite, Carbon 35 (3) (1997)
341   393–401.

342 [3] H. Jiang, J. Wang, S. Wu, B. Wang, Z. Wang, Pyrolysis kinetics of
343   phenol-formaldehyde resin by non-isothermal thermogravimetry, Car-
344   bon 48 (2010) 1527–1533.

345 [4] H. Jiang, J. Wang, S. Wu, Z. Yuan, Z. Hu, R. Wu, Q. Liu, The pyroly-
346   sis mechanism of phenol formaldehyde resin, Polymer Degradation and
347   Stability 97 (2012) 1527–1533.

[5] B. S. Venkatachari, G. C. Cheng, R. P. Koomullil, A. Ayasoufi, Computational tools for re-entry aerothermodynamics: Part II. Surface ablation, AIAA paper 2008-1218.

[6] N. N. Mansour, J. Lachaud, T. E. Magin, J. de Muelenaere, Y.-K. Chen, High-fidelity charring ablator thermal response model, AIAA Paper 2011-3124.

[7] Y.-K. Chen, F. Milos, Effects of non-equilibrium chemistry and darcy-forchheimer flow of pyrolysis gas for a charring ablator, AIAA paper 2011-3122.

[8] A. Bennett, D. R. Payne, R. W. Court, Quantitative pyrolytic and elemental analysis of a phenolic resin, AIAA Paper 2013-0183.

[9] H.-W. Wong, J. Peck, R. A. Edwards, G. Reinisch, J. Lachaud, N. N. Mansour, Measurement of pyrolysis products from phenolic polymer thermal decomposition, AIAA Paper 2014-1388.

[10] E. M. Suuberg, M. Wojtowicz, J. M. Calo, Some aspects of the thermal annealing process in a phenol-formaldehyde resin char, Carbon 27 (3) (1989) 430–441.

[11] M. S. Chetan, R. S. Ghadage, C. R. Rajan, V. G. Gunjikar, Thermolysis of orthonovolacs. part 1. phenol-formaldehyde and m-cresol formaldehyde resins, Thermochimica Acta 228 (1993) 261–270.

[12] L. Costa, L. R. de Montelera, G. Camino, E. D. Weil, E. M. Pearce, Structure-charring relationship in phenol-formaldehyde type resins, Polymer Degradation and Stability 56 (1997) 23–35.

371 [13] C. A. Lytle, W. Bertsch, M. McKinley, Determination of novolac resin
372   thermal decomposition products by pyrolysis-gas chromatography, Jour-
373   nal of Analytical and Applied Pyrolysis 45 (1998) 121–131.

374 [14] M. P. R. Rao, B. S. M. Rao, C. R. Rajan, R. S. Ghadage, Thermal degra-
375   dation kinetics of phenol-formaldehyde resins, Polymer Degradation and
376   Stability 61 (1998) 283–288.

377 [15] J.-M. Lin, C.-C. M. Ma, Thermal degradation of phenolic resin/silica
378   hybrid beramers, Polymer Degradation and Stability 69 (2000) 229–235.

379 [16] K. Ouchi, Infra-red study of structural changes during the pyrolysis of
380   a phenol-formaldehyde resin, Carbon 4 (1966) 59–66.

381 [17] Y. Yamashita, K. Ouchi, A study on carbonization of phenol-
382   formaldehyde resin labelled with deuterium and c13, Carbon 19 (1981)
383   89–94.

384 [18] C. Morterra, M. J. D. Low, Ir studies of carbons - vii. the pyrolysis of a
385   phenol-formaldehyde resin, Carbon 23 (5) (1985) 525–530.

386 [19] Z. Lausevic, S. Marinkovic, Mechanical properties and chemistry of car-
387   bonization of phenol formaldehyde resin, Carbon 24 (5) (1986) 575–580.

388 [20] M. V. Alonso, M. Oliet, J. C. Dominguez, E. Rojo, F. Ro-
389   driguez, Thermal degradation of lignin-phenol-formaldehyde and
390   phenol-formaldehyde resol resins, Journal of Thermal Analysis and
391   Calorimetry 105 (2011) 349–356.

392 [21] G. F. Sykes, Decomposition characteristics of a char-forming phenolic
393   polymer used for ablative composites, Technical report, NASA (1967).

394 [22] G. F. Sykes, Thermal cracking of phenolic-nylon pyrolysis products on
395   passing through a heated char, Technical report, NASA (1970).

396 [23] R. Lum, W. Wilkins, M. Robbins, A. M. Lyons, R. P. Jones, Thermal
397   analysis of graphite and carbon-phenolic composites by pyrolysis-mass
398   spectrometry, Carbon 21 (2) (1983) 111–116.

399 [24] J. Hetper, M. Sobera, Thermal degradation of novolac resins by
400   pyrolysis-gas chromatography with a movable reaction zone, Journal
401   of Chromatography A 833 (1999) 277–281.

402 [25] M.-F. Grenier-Loustalot, G. Raffin, B. Salino, O. Paisse, Phenolic resins
403   part 6. identifications of volatile organic molecules during thermal treat-
404   ment of neat resols and resol filled with glass fibers, Polymer 41 (2000)
405   7123–7132.

406 [26] M. Sobera, J. Hetper, Pyrolysis-gas chromatography-mass spectrometry
407   of cured phenolic resins, Journal of Chromatography A 993 (2003) 131–
408   135.